All Fibre Continuous Wave Supercontinuum Sources for fibre sensing purposes

S. Martín-López*[a], P. Corredera[a], L. Abrardi[a], A. Carrasco-Sanz[a], F. Rodríguez-Barrios[a], M.L. Hernanz[a] and M. González-Herráez[b]
[a] Instituto de Física Aplicada, CSIC, Madrid, Spain;
[b] Departamento de Electrónica, UAH, Alcalá de Henares, Spain

Abstract - A supercontinuum light source is a wideband source obtained as the result of the broadening of a spectrally narrow pump source in a nonlinear medium. The high spectral brightness, large spectral width, tailored wavelength band of emission, and coherence make supercontinuun sources (SC) very attractive for photonics applications. The SCs generated with continuous wave (CW) pumps have the additional property that they present much higher spectral power density than the ones generated with pulsed pumps. We present three different supercontinuun sources tailored with conventional telecommunications fibers in order to obtain high power emission in the 1300 and 1550 nm spectral regions. We show that the spectral width, spectral shape and brightness of the supercontinua can be designed by a precise selection of the dispersion proprieties of the fibers used. This properties convert this type of sources in a very interesting candidate to be used in fiber sensing and photonic applications, for instance to avoid the need of amplification in the interrogation of remote Bragg gratings or to improve the resolution and dynamic range of optical coherence tomography setups.

Keywords – supercontinuum, broadband sources, optical coherence tomography.

I. INTRODUCTION

A supercontinuum light source (SC) is a wideband source obtained as the result of the broadening of a spectrally narrow pump source in a nonlinear medium. Research on SC generation in optical fibers still attracts much attention both from fundamental and applied viewpoints [1]. So far, wide SCs (up to two octave spanning) has been reported and soon considered as a promising tool for metrology, biomedical and telecommunication applications, due to their high spectral brightness compared with traditional broadband light sources (incandescent or fluorescent sources). Primary results were obtained with pulsed pump [1],[2],[3],[4] launched in Photonic Cristal Fibers (PCF), in tapered fibers [5] or in classical telecommunication fibers [8]. The basic principles of SC generation in the continuous wave (CW) regime are similar to those of the pulsed regime, except that the initial CW field is first converted into a train of ultra-short pulses whose duration, peak power and repetition rate are not constant [6],[7],[8],[9]. Since different pulses propagate in the fiber, the possibility to generate new spectral components and the location of these new frequencies depends on the characteristics of each pulse. The overall spectrum seen at the fiber output can be seen as the averaging of many of these individual spectra generated along the fiber. As a consequence, SCs obtained in the CW regime are usually smoother and more stable than those obtained in the pulse regime. From a practical point of view, recent advances in high power CW fiber lasers allow the achievement of compact and robust all-fiber SC light sources with higher Power Spectral Density (PSD) compared with pulsed SCs [6][9][10][11][12][13]. This, of course, extends their field of application in such diverse fields as spectroscopy, pulse compression, the design of tunable ultra fast femtosecond laser sources, and of course, metrology. In this last field, the properties of supercontinuum sources as their high spectral brightness compared with traditional broadband light sources (incandescent or discharge sources), large spectral width, tailored wavelength band, and coherence are very interesting.

In this paper we show some of the all fibre CW SCs that we have developed and the possibilities to modify their properties to optimize them for different applications like optical coherence tomography (OCT), spectrophotometry or sensing. In the next section we will describe the generation of our first CW SC source and we will explain its good properties compared with pulsed SC. In section III we will depict the generation of a CW SC in the region of 1300 nm. In section IV we will describe how to obtain SC sources with a controlled spectral width to make them much more appropriate for specific applications, in which the use of a broadband source with a fix spectral width and a high power spectral density is required, as OCT.

II. CW SUPERCONTINUUM SOURCES

The basic principles of SC generation in the continuous wave regime are similar to those of the pulsed regime for anomalous group velocity dispersion (GVD) regime pumping. In the case of CW pumping the initial field is first converted into a train of ultra-short pulses whose duration, peak power and repetition rate are not constant [1],[8]. Since different pulses propagate in the fibre, the possibility to generate new spectral components and the location of these new frequencies depends on characteristics of each pulse. The overall spectrum seen at the fibre output can be seen as the averaging of many of these individual spectra generated along the fibre. As a consequence, SCs obtained in the CW regime are usually smoother and more stable than those obtained in the pulse regime. This is one of the main reasons why the CW SCs are more adequate for metrological purposes than pulsed ones.

In our first experiments, a Raman fibre laser emitting around 1455 nm was used, i.e. in the vicinity of the zero dispersion wavelength (λ_0) of a non zero dispersion wavelength fibre

(NZDF) (1453 nm) [14],[15] (see Fig. 1). With this configuration we obtained a light source with more than 200 nm of spectral bandwidth measured at 20 dB from the peak, with a flat spectral profile and a high power density (>0 dBm/nm). For low pump power levels (Pp ≈ 0.3 W), the output spectrum exhibits a clear signature of the influence of Four Wave Mixing (FWM) through the generation of two nearly symmetric modulational instability (MI) sidebands around the pump frequency.

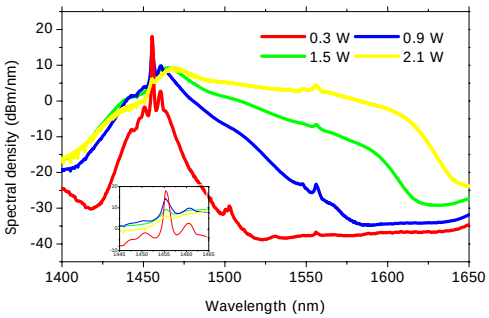

Fig. 1: Supercontinuum spectra generated with a pump Raman laser (1455 nm) at different input powers in 6.7 km of non zero dispersion fibre (NZDF).

The asymmetry in the intensity of those sidebands is caused by SRS amplification of the longer wavelengths and attenuation of the shorter ones. For higher pump powers, the effective FWM and Raman gains increase, which leads to a continuous broadening of the generated spectrum. Note that this broadening mainly occurs on the long wavelength side of the pump wave but short wavelength components are also significantly generated. Beyond a pump power Pp ≈ 1.5 W, all the pump energy is transferred to the SC and nearly complete pump depletion is achieved (see the inset of Fig. 1). At this point, our SC has a 20-dB bandwidth of over 200 nm and a peak power spectral density > 8 dBm/nm. We must point out that, apart from the initial MI sidebands, our SC spectrum exhibits a very smooth spectral structure at all pump power levels and that it broadens very regularly with increasing pump powers.

The long-term stability of this source was evaluated with spectral acquisitions each 40 s during 1 h. The standard deviation of the results from the mean supercontinuum spectrum was computed for each wavelength and normalized to the corresponding mean detected power. The results are presented in linear units in Fig. 2 (restricted to the wavelength range of the 20-dB SC width). We can see that the stability of the source is relatively flat and better than 1% around the pump wavelength (from 1410 to 1518 nm) while it grows slightly for the wavelengths of the first Raman order (around 1565 nm). Curiously, around these wavelengths there is a strong ripple in the standard deviation of the recorded traces. The origin of this ripple is difficult to explain, but it seems associated with the peak-like feature present in the supercontinuum spectrum around 1560 nm. This peak appears already in the pump spectrum and is possibly originated due to four-wave mixing processes within the RFL. For the longer wavelengths of the supercontinuum (>1600 nm) there is a strong growth of the standard deviation of the spectral density. An explanation of this behavior can be found if we track the evolution of the recorded power spectral density with time.

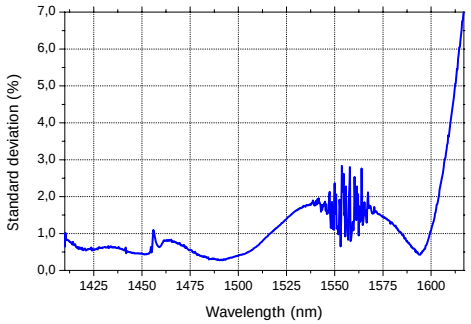

Fig. 2: Standard deviation of the power detected for each wavelength, in linear units.

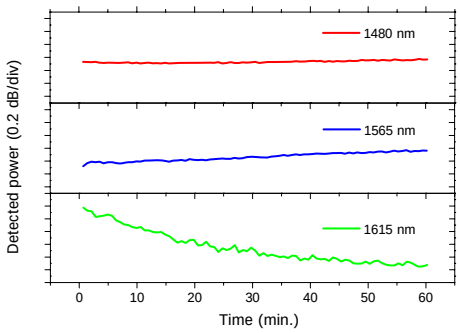

Fig. 3: Evolution of the detected power as a function of time for three specific wavelengths.

In Fig. 3 we show in detail the evolution of the detected powers for three specific wavelengths over the one hour test. At 1480 nm, the detected power remains stable within ±0.03 dB. At 1565 nm, there is a positive drift in the detected power with time (+0.2 dB), while at 1615 nm (already in the limit of the 20-dB band) the detected power becomes smaller with time (-0.9 dB). While the overall power contained in the supercontinuum remains unchanged (this is checked by direct numerical integration of the different spectra acquired with time), a spectral redistribution of the power has happened. This gentle drift is not caused by wavelength changes in the RFL and neither by temperature changes of the fiber environment, since the fiber was properly isolated. Additionally, several consecutive tests have shown that the drift is repetitive. The origin of this small drift is unclear, but it might be related to some small intrinsic heating of the fiber due to the ~0.6 watts of power lost by Rayleigh scattering in the fiber. This residual heating of the fiber would cause small changes in the fiber parameters (chromatic dispersion and nonlinear coefficient). Due to the special nature of the supercontinuum generation process, the edges of the supercontinuum are strongly sensitive to small changes in the

chromatic dispersion coefficient, the nonlinear coefficient and the Raman gain of the fiber [9],[14],[15],[16]. A close look at Fig. 3 suggests that the drift tends to diminish with time. It might be necessary, thus, to stabilize the source for some time before usage if a very high stability is required.

III. CW SC AT 1300NM REGION

Using the same principle described in the previous section, we developed other broadband sources in a tunable spectral range and with a tunable spectral width. For this purpose we used the dependence of the SC morphology with the dispersion parameters of the optical fibre used. If we tune the pump laser wavelength and we choose an appropriate fibre concatenation to have an optimal dispersion profile, we can obtain a broader and smoother supercontinuum spectrum, centered in a different spectral region (1300 nm).

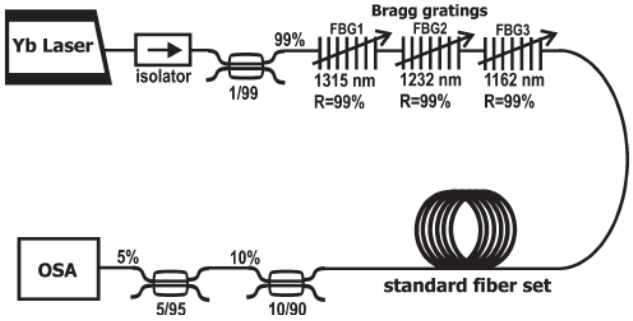

Fig. 4: Experimental setup. Yb laser: Tunable Ytterbium-doped fiber laser emitting at 1104 nm. FBG: Fiber Bragg Gratings. OSA: Optical Spectrum Analyzer. The standard fiber set is made up of four fibers whose details can be seen in Table I.

To obtain efficient spectral broadening from CW laser in conventional fibers one needs to have the pump tuned at wavelengths in which the fiber exhibits small anomalous dispersion. Standard optical fibers have λ_0 around 1310 nm. Thus, to enable SC emission, we need to shift most of the laser power from 1100 nm to >1310 nm (where standard fibers exhibit small anomalous dispersion) to efficiently induce modulation instability (MI). In order to do this, we insert a cascade of Fiber Bragg Grating mirrors (FBGs) between the pump and the fiber set. In Fig. 4 we depict the experimental setup. We developed a home-made Raman source from a commercial Ytterbium laser and an array of fibre Bragg gratings (see Fig. 4). The output of the Ytterbium laser is single-mode, tunable from 1080 nm to 1110 nm and an output power from 0.57 W to 20 W [17]. The FBGs arrangement allows to shift the laser emission at the desired wavelength without the need of a cavity. The FBGs have reflectivity >99% in all cases and total loss of 0.8 dB. Their bandwidths are centered at 1162 nm, 1232 nm and 1315 nm and have reflection bandwidths of 1.47 nm, 1.73 nm and 8.00 nm, respectively. FBG at 1315 nm has its maximum and minimum reflection at 1312 nm and 1320 respectively.

The non-linear medium is made of a set of four standard single-mode fibers (SMF) of different λ_0 and lengths. We used two different fibre configurations with the purpose of obtaining a SC spectrum as flat and wide as possible. In Table I we show properties of the four initial fibres.

TABLE I
PROPERTIES OF THE SET OF OPTICAL FIBERS USED IN THE EXPERIMENT

	λ_0 nm	S_0 ps/nm^2/km	α (1310 nm) dB/km	L km	D (1315 nm) ps/nm/km
Fibre 1	1302	0.085	0.35	6.0	1.02
Fibre 2	1307	0.087	0.33	8.0	0.60
Fibre 3	1311	0.083	0.34	2.0	0.33
Fibre 4	1312	0.085	0.34	2.0	0.23

In Fig. 5 we depict the output spectrum for different pump powers. The values of pump power were measured at the input of the fibre set. The first Raman peak at 1162 nm appears when the input power takes the value of 1.16 W. At 2.37 W the second Raman peak at 1232 nm is also present. At this stage, depletion of the spectral lines at 1104 nm and 1162 nm also begins to occur. At input power level of 4.15 W the spectral lines at 1104 nm and 1162 nm undergo almost full depletion and a peak at 1312 nm is clearly visible. When the input power amounts to 4.73 W the spectral broadening starts to take place around 1315 nm. At power levels higher than 4.5 W the spectral broadening around 1315 nm starts to take place and another Raman peak appears at 1397 nm. MI-induced soliton fission and Raman shift is also evident from the appearance of a smooth red-shifted tail in the pump spectrum.

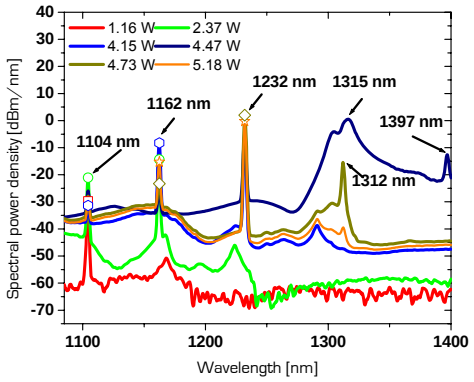

Fig. 5: Output spectra for different input powers. Evolution of the pump broadening around 1315 nm.

In Fig.6 we show the SC spectrum obtained for two different fiber configurations. The first one (solid circles) makes use of the set of fibers shown in Table I arranged in dispersion decreasing order. The input power is 8.17 W, while the SC output power is 1.36 W. The output spectrum spans over 232.5 nm as measured at 20 dB from the highest peak and exhibits >0 dBm/nm spectral density over 200 nm. The Raman-induced asymmetric broadening towards longer wavelengths is clearly visible. A significant feature is the appearance of a peak at 1397

nm and a strong power transfer to the region between 1400 and 1450 nm, which is caused by forward Stimulated Raman Scattering (SRS). To our knowledge, this is the broadest cw-pumped SC spectrum obtained by the only use of standard optical fibers. We saw that, as we expected, the decreasing dispersion configuration gives rise to the wider spectrum compared to other configurations (random dispersion and increasing dispersion distribution).. In a further demonstration of the possibilities offered by dispersion management, a DSF is added at the end of the optimum fiber arrangement in such a way as to keep a decreasing-dispersion configuration. This fiber was 2 km long and had its λ_0 at 1417 nm. Since a significant part of the SC power generated lied at wavelengths slightly above the λ_0 of this fiber, we expected that the insertion of this fiber would stimulate soliton fission in this spectral region and provide further spectral broadening [1],[9],[18],[19]. As can be seen, this arrangement improves the spectral width of our SC. In this case (achieved for 8.17 W of input pump power), the SC spectrum spans > 260 nm, as measured at 20 dB from the highest peak; it has an output power of 0.840 W and exhibits > 0 dBm/nm spectral density over 214 nm.

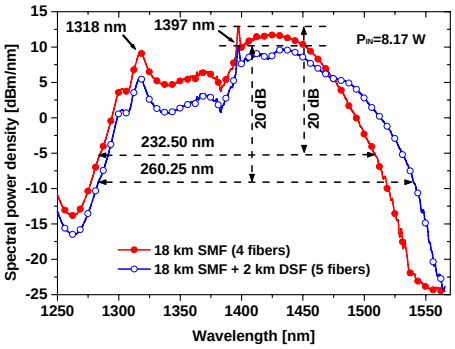

Fig.6: Supercontinuum spectra for two different fibre configurations.

IV. SC SPECTRAL WIDTH CONTROL

For some applications it would be desired to have a fixed spectral width in the SC and to increase the power spectral density (PSD) proportionally to the input pump power. For this purpose we developed an experimental setup in which we pumped a flat dispersion fibre (FDF) with a power and wavelength tunable fibre ring laser. We realized a wavelength-tunable Erbium-doped fiber ring laser delivering a maximum power of 7 W and a spectral width (FWHM) of 0.08 nm (see Fig. 7). The dispersion curve of the FDF has been measured between 1470 nm and 1570 nm using the phase shift method [20] (see Fig. 8). By extrapolating these measurements, we found that the first ZDW is at 1390 nm and the second one at 1652 nm. We demonstrated experimentally that beyond a certain pump power, the width of the SC source remains fixed, and the PSD of the SC grows with the pump power.

The mechanisms involved in the generation of this SC are the same that in Ref. [21] except that the pump wavelength is located at 1550 nm rather than 1064 nm and that we used a very long FDF (6 km) rather than a PCF of a few tens meters.

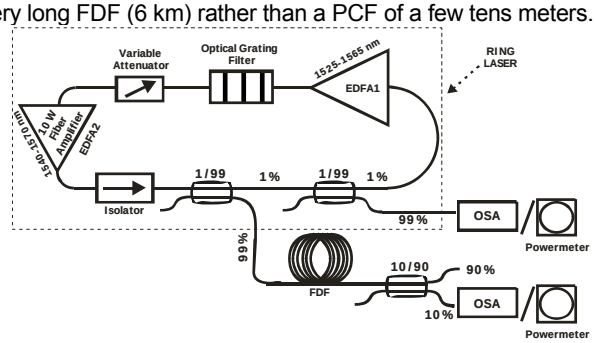

Fig. 7: Experimental setup. EDFA: erbium-doped fiber amplifier, FDF: flat dispersion fiber, OSA: optical spectrum analyzer.

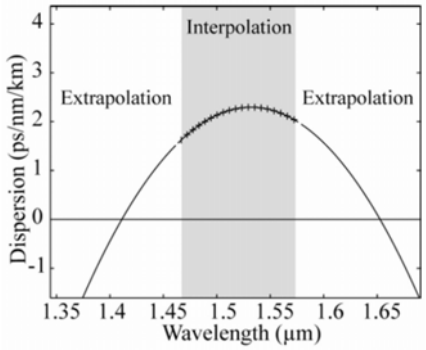

Fig. 8: Dispersion curve of the 6 km FDF. The values beyond 1570 nm and under 1470 nm are extrapolated from the measured data

At the beginning the MI process generates temporal spikes of a few picoseconds duration. These quasi-solitonic pulses are not stable under higher order effects and Stimulated Raman Scattering and they split into fundamental solitons, releasing energy as dispersive waves (DWs). Subsequently, the SRS effect shifts these fundamental solitons towards longer wavelengths. Because of the special characteristics of this fiber, the frequency shift is stopped by the second ZDW. Around this wavelength, a balance is achieved between the red shift due to SRS and the blue shift due to spectral recoil when the dispersion slope of the fiber is negative [22]. The SC is bounded by two dispersive waves whose spectral position is defined by this phase matching condition [9],[23]:

$$\Delta\beta = \beta(\omega_P) - \beta(\omega_{DW}) = \\ = \frac{\gamma P_P}{2} - \sum_{n\geq 2}^{n=12} \frac{(\omega_P - \omega_{DW})^n}{n!} \beta_n(\omega_P) = 0 \quad (1)$$

Where $\beta(\omega_P)$ and $\beta(\omega_{DW})$ represent the propagation constants at the angular frequency of the pump (ω_P) and the dispersive wave (ω_{DW}) respectively. In optical fibers having a single ZDW, DWs are blue shifted [23] while in optical fibers with two ZDWs, two bands of DWs appear: One is blue shifted and appears below

the first ZDW (λ_{01}~1430 nm) (DW1); the other is red shifted and appears above the second ZDW (λ_{02}~1650 nm) (DW2) [4].

In our experiment we generated a reasonably flat, spectrally-bounded SC spanning from 1550 nm to 1700 nm. The spectral width of the source is shown to be constant between 3 and 6 W. Over this range, the increase in input power is directly translated in an increase in the output PSD (see Fig. 9(a)) [9].

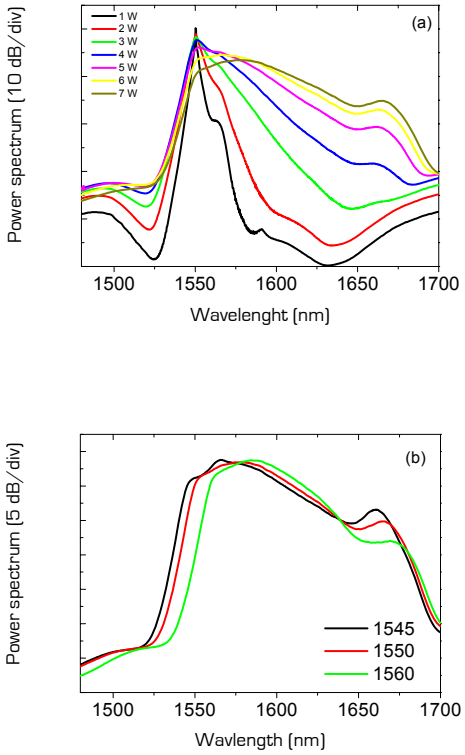

Fig.9: Spectra measured at the output of the 6 km FDF: (a) Output spectra at different input powers for the pump wavelength of 1550 nm. (b) Output spectral at different pump wavelengths for an input pump power of 7 W.

As it was expected, the spectral bounding of the SC is achieved in this fiber between the pump wavelength at 1550 nm and the second DW generated at about 1675 nm. This DW should be caused by solitons which are shifted just below the second ZDW. As it can be seen, the spectral edges of the SC remain constant for input powers varying from 4 W up to 7 W. The position of the second DW does not depend on the pump power. As a consequence, for a fixed pump wavelength we are able to control the average power spectral density (APSD) of the SC by simply tuning the pump power. For instance, when pumping at 1550 nm, an increase in the input pump power from 4 to 7 W leads to a raise in the APSD of the SC from 0.96 dBm/nm to 1.87 dBm/nm. It must be noted that the increase in APSD is not linear with the input pump power. This is probably due to the fact that the losses in the fiber are strongly wavelength-dependent (they are higher for longer wavelengths). When the pump power is increased, the longer wavelength part of the SC is being enhanced. The frequencies lying in this part of the spectrum experience more losses than the wavelengths lying closer to 1550 nm.

The output spectra obtained at three different pump wavelengths are represented in Fig. 9(b). The upper limit of the SC remains nearly constant, even if we observed a slight modification of the position of the peak around 1670 nm. It is difficult to determine if this peak is mainly due to the SRS effect (the spectral shift from the pump is around the SRS shift, 106 nm at 1550 nm) or to the second DW.

IV. CONCLUSIONS

We have presented a summary of some of the most interesting experiments done in our laboratory, specially focused on how to develop all fibre CW SC with desired spectral profile and power density. First we have shown how to generate a CW SC in a standard fibre and its very good properties of low noise and high stability, which make it very appropriate for sensing purposes and spectral characterization of different devices. We have demonstrated pump spectral broadening and supercontinuum generation spanning more than 232 nm in the spectral range of 1.2-1.5 μm. This has been achieved by pumping a concatenation of conventional fibers with an Yb-doped fiber laser and a frequency-selective reflective structure that seeds supercontinuum emission at 1315 nm, in the regime of small anomalous dispersion of the fibers. We believe that such a SC profile is very promising for high power density, all-fiber SC applications and seems particularly interesting for ultrahigh resolution OCT. We have presented our experimental work on SC generation under CW pumping for spectrally bounded supercontinuum generation by using a fiber with 2 ZDWs. We achieved a quite flat SC spanning from 1550 nm to 1700 nm with an average PSD of 10 mW/nm. These sources are of primary interest for optical coherence tomography applications. All these properties make these sources appropriated for different applications like spectroscopy, filter measurement and characterization, optical coherence tomography and sensors calibration using monochromators.

V. ACKNOWLEDGEMENTS

We acknowledge financial support from the Ministerio de Educacion y Ciencia through projects TEC2006-09990-C02-01 and TEC2006-09990-C02-02, the support from CSIC through project MeDIOMURO, the support from the Comunidad Autonoma de Madrid through the projects FUTURSEN S-0505/AMB/000374 and FACTOTEM S-0505/ESP/000417, and the support from Social European Fund through the grant program I3P of CSIC.

VI. REFERENCES

[1] J. M. Dudley, G. Genty, and S. Coen, “Supercontinuum generation in photonic crystal fiber,” Rev. Mod. Phys., vol. 78, no. 4, pp. 1135–1184, 2006.

[2] J. K. Ranka, R. S. Windeler, and A. J. Stentz, ”Visible continuum generation in air-silica microstructure optical fibers with anomalous dispersion at 800 nm”, Optics Letters, vol 25, pp 27-27, 2000.

[3] 4. S. Coen, A. H. L. Chau, R. Leonhardt, J. D. Harvey, J. C. Knight, W. J. Wadsworth, and P. S. J. Russell, "Supercontinuum generation by stimulated Raman scattering and parametric four-wave mixing in photonic crystal fibers ," Journal of Optical Society of America B, vol 19, pp 753-764, 2002.

[4] G. Genty, M. Lehtonen, and H. Ludvigsen, "Effect of cross-phase modulation on supercontinuum generated in microstructured fibers with sub-30 fs pulses," Optics Express, vol 12, pp 4614-4624, 2004.

[5] 7. T. A. Birks, W. J. Wadsworth, and P. S. J. Russell, "Supercontinuum generation in tapered fibers," Optics Letters, vol 25, pp 1415-1417, 2000.

[6] S. Kobtsev and S. Smirnov, "Modelling of high-power supercontinuum generation in highly nonlinear, dispersion shifted fibers at CW pump," Optics Express, vol 13, pp 6912-6918, 2005.

[7] M. H. Frosz, O. Bang, and A. Bjarklev "Soliton collision and Raman gain regimes in continuous-wave pumped supercontinuum generation," Optics Express vol 14, pp 9391-9407, 2006.

[8] A. Mussot, E. Lantz, H. Maillotte, T. Sylvestre, C. Finot, and S. Pitois, "Spectral broadening of a partially coherent CW laser beam in single-mode optical fibers," Optics Express vol 12, pp 2838-2843, 2004.

[9] S. Martin-Lopez, L. Abrardi, P. Corredera, M. Gonzalez-Herraez, A. Mussot, “Spectrally-bounded continuous-wave supercontinuum generation in a fiber with two zero-dispersion wavelengths”, Optics Express vol 16, pp 6745-6755, 2008.

[10] A. K. Abeeluck, C. Headley, and C. G. Jørgensen, "High-power supercontinuum generation in highly nonlinear, dispersion-shifted fibers by use of a continuous-wave Raman fiber laser," Optics Letters, vol. 29, pp 2163-2165, 2004.

[11] T. Sylvestre, A. Vedadi, H. Maillotte, F. Vanholsbeeck, and S. Coen, "Supercontinuum generation using continuous-wave multiwavelength pumping and dispersion management," Optics Letters, vol 31, pp 2036-2038, 2006.

[12] A. V. Avdokhin, S. V. Popov, and J. R. Taylor, "Continuous-wave, high-power, Raman continuum generation in holey fibers " Optics Letters, vol. 28, pp 1353-1355, 2003.

[13] J. C. Travers, S. V. Popov, J. R. Taylor, H. Sabert, and B. Mangan, "Extended Bandwidth CW-Pumped Infra-Red Supercontinuum Generation in Low Water-Loss PCF," in Conference on Lasers and Electro-Optics/Quantum Electronics and Laser Science and Photonic Applications Systems Technologies, Technical Digest (CD) (Optical Society of America, 2005), paper CFO4.

[14] M.Gonzalez-Herraez, S. Martin-Lopez, P. Corredera, M. L. Hernanz, and P. R. Horche, ”Supercontinuum generation using a continuous-wave Raman Fiber laser”, Optics Communications, vol 226, pp 323-328 ,2003.

[15] F. Vanholsbeeck, S. Martín-López, M. González-Herráez, and S. Coen, “The role of pump incoherence in continuous-wave supercontinuum generation”, Optics Express vol 13, pp 6615-6625, 2005.

[16] S. Martin-Lopez, M.I Gonzalez-Herraez, A. Carrasco-Sanz, F. Vanholsbeeck, S. Coen, H. Fernandez, J. Solis, P. Corredera and M.L. Hernanz, “Broadband spectrally flat and high power density light source for fibre sensing purposes”, Measurement Science Technology, vol 17, pp 1014-1019, 2006.

[17] L. Abrardi, S. Martin-Lopez, A. Carrasco-Sanz, P. Corredera, M. L. Hernanz and M. Gonzalez-Herraez, “Optimized All-Fiber Supercontinuum Source at 1.3 μm Generated in a Stepwise Dispersion-Decreasing-Fiber Arrangement”, Journal of Lightwaves Technologies, vol 25, pp 2098-2102, 2007.

[18] A. V. Husakou and J. Hermann, “Supercontinuum generation, four-wave mixing, and fission of higher-order solitons in photonic crystal fibers,” Journal of Optical Society of America B, vol. 19, no. 9, pp. 2171–2182, 2002.

[19] J. Hermann, U. Griebner, N. Zhavoronkov, A. Husakou, D. Nickel, J. C. Knight, W. J. Wadsworth, P. S. J. Russel, and G. Korn, “Experimental evidence for supercontinuum generation by fission of higher-order solitons in photonic fibers,” Physical Review Letters, vol. 88, no. 17, pp. 173 901.1–173 901.4, 2002

[20] B. Costa, D. Mazzoni, M. Puleo, and E. Vezzoni, “Phase-shift tecnique for the measurement of chromatic dispersion in optical fibers using leds,” IEEE Journal of Quantum Electronics, vol 18, pp 1509–1515, 1982.

[21] A. Mussot, M. Beaugeois, M. Bouazaoui, and T. Sylvestre, "Tailoring CW supercontinuum generation in microstructured fibers with two-zero dispersion wavelengths," Optics Express, vol 15, pp 11553-11563, 2007

[22] D. V. Skryabin, F. Luan, J. C. Knight, and P. S. J. Russell, “Soliton self-frequency shift cancellation in photonic crystal fibers,” Science, vol 301, pp 1705–1708, 2003.

[23] N. Akhmediev and M. Karlsson, ”Cherenkov radiation emitted by solitons in optical fibers,” Physical Review A, vol 51, pp 2602-2607, 1995.